HOKKAIDO UNIVERSITY

Title	Effects of dissolved oxygen and pH on nitrous oxide production rates in autotrophic partial nitrification granules
Author(s)	Rathnayake, Rathnayake M.L.D.; Oshiki, Mamoru; Ishii, Satoshi et al.
Citation	Bioresource Technology, 197, 15-22 https://doi.org/10.1016/j.biortech.2015.08.054
Issue Date	2015-12
Doc URL	https://hdl.handle.net/2115/67732
Rights	© 2015, Elsevier. Licensed under the Creative Commons Attribution-NonCommercial-NoDerivatives 4.0 International http://creativecommons.org/licenses/by-nc-nd/4.0/
Rights(URL)	https://creativecommons.org/licenses/by-nc-nd/4.0/
Type	journal article
File Information	Rathnayake 2015 Bioresource Technology 197 15-22.pdf



Hokkaido University Collection of Scholarly and Academic Papers : HUSCAP

Effects of dissolved oxygen and pH on nitrous oxide production rates in autotrophic partial nitrification granules

Rathnayake M.L.D. Rathnayake[a], Mamoru Oshiki[a,b], Satoshi Ishii[a,c], Takahiro Segawa[d], Hisashi Satoh[a,*], Satoshi Okabe[a]

[a] Division of Environmental Engineering, Faculty of Engineering, Hokkaido University, North-13, West-8, Sapporo 060-8628, Japan

[b] Department of Civil Engineering, Nagaoka National College of Technology, 1603-1 Kamitomioka, Nagaoka, Niigata 940-2188, Japan

[c] Department of Soil, Water, and Climate BioTechnology Institute, University of Minnesota, 140 Gortner Laboratory of BioChemistry, 1449 Gortner Avenue, St. Paul, MN 55108-1095, U.S.A.

[d] Transdisciplinary Research Integration Center, National Institute of Polar Research, 10-3 Midori-cho, Tachikawa, Tokyo 190-8518, Japan

E-mail addresses:

Rathnayake M.L.D. Rathnayake – englashi@gmail.com

Mamoru Oshiki – oshiki@nagaoka-ct.ac.jp

Satoshi Ishii – ishi0040@umn.edu

Takahiro Segawa – segawa@nipr.ac.jp

Hisashi Satoh – qsatoh@eng.hokudai.ac.jp

Satoshi Okabe – sokabe@eng.hokudai.ac.jp

*Corresponding author

Hisashi Satoh, Division of Environmental Engineering, Faculty of Engineering, Hokkaido University, North-13, West-8, Sapporo 060-8628, Japan

Tel: +81-(0)11-706-6277; Fax: +81-(0)11-706-6277; E-mail: qsatoh@eng.hokudai.ac.jp

Abstract

The effects of dissolved oxygen (DO) and pH on nitrous oxide (N_2O) production rates and pathways in autotrophic partial nitrification (PN) granules were investigated at the granular level. N_2O was primarily produced by betaproteobacterial ammonia-oxidizing bacteria, mainly *Nitrosomonas europaea*, in the oxic surface layer (< 200 μm) of the autotrophic PN granules. N_2O production increased with increasing bulk DO concentration owing to activation of the ammonia (*i.e.*, hydroxylamine) oxidation in this layer. The highest N_2O emissions were observed at pH 7.5, although the ammonia oxidation rate was unchanged between pH 6.5 and 8.5. Overall, the results of this study suggest that *in situ* analyses of PN granules are essential to gaining insight into N_2O emission mechanisms in a granule.

Keywords: N_2O emissions; autotrophic partial nitrification granule; dissolved oxygen effect; 16S rRNA gene deep sequencing; N_2O microsensor

Abbreviations: A2O: anaerobic-anoxic-oxic; AOR: ammonium oxidation rate; ATU: allylthiourea; COD: chemical oxygen demand; DO: dissolved oxygen; FISH: fluorescence in situ hybridization; FNA: free nitrous acid; NER: nitrous oxide emission rate; NH_2OH: hydroxylamine; N_2O: nitrous oxide; NOH: nitrosyl radical; OTU: operational taxonomic unit; PCR: Polymerase chain reaction; PN: partial nitrification; R(N_2O): net volumetric emission rates of nitrous oxide; SBR: sequencing batch reactor; VSS: volatile suspended solids

1. Introduction

Nitrogen removal from wastewater via a combination of partial nitrification (PN) and anaerobic ammonium oxidation (anammox) processes has recently drawn attention as an alternative to conventional nitrification-denitrification processes (Castro-Barros et al., 2015; Cho et al., 2011; Kampschreur et al., 2008; Okabe et al., 2011a). The advantages of the PN-anammox process over conventional processes include lack of a need for external organic carbon, low oxygen demand, small sludge production, and low emissions of carbon dioxide (CO_2) (Kartal et al., 2010). Therefore, this technology enables low cost removal of nitrogen from wastewater while using little energy (Kartal et al., 2010). In addition, use of granular sludge and biofilm for PN instead of activated sludge flocs has attracted attention because of good sludge settleability, long-term retention of slow-growing nitrifying bacteria in a reactor and high specific nitrification rate (Zheng et al., 2005).

Nitrous oxide (N_2O) can be produced in PN granular sludge processes, which poses a significant threat to the ozone layer (Desloover et al., 2012) and is an important greenhouse gas that has a global warming potential about 300 times greater than that of CO_2. N_2O emissions were higher in a PN reactor than a full nitrifying reactor (Wei et al., 2014), probably owing to high nitrite (NO_2^-) concentrations and dissolved oxygen (DO)-limited conditions (Castro-Barros et al., 2015; Ishii et

al., 2014; Pijuan et al., 2014; Rathnayake et al., 2013; Wei et al., 2014). During biological nitrogen removal processes in wastewater treatment, N_2O can be produced via three primary microbiological pathways.

(1) As a byproduct of nitrification: During this process, nitrosyl radical (NOH) is produced as an intermediate during oxidation of hydroxylamine (NH_2OH) into NO_2^- (Igarashi et al., 1997). Next, NOH is biologically transformed into NO and then N_2O, or chemically broken down to N_2O (Poughon et al., 2001).

(2) As an intermediate during denitrification (*i.e.*, reduction of NO_2^- to N_2) by heterotrophic bacteria (Lu and Chandran, 2010).

(3) By ammonia-oxidizing bacteria (AOB) (*i.e.*, nitrifier denitrification) under high NO_2^- or oxygen limiting conditions (Wrage et al., 2001).

The N_2O emission factors range from 1.5% of the ammonium (NH_4^+) oxidized (Rathnayake et al. 2013) to 19% of the nitrogen oxidized (Pijuan et al., 2014). Such variety in N_2O emission rates (NERs) could be explained by the different responses of N_2O producing reactions (e.g., NH_2OH oxidation, nitrifier denitrification and heterotrophic denitrification) to physicochemical parameters such as DO, NH_4^+ and NO_2^- concentrations, pH, temperature and chemical oxygen demand (COD)/nitrogen ratio (Kampschreur et al., 2009; Okabe et al., 2011b). Accordingly, many studies have been conducted to investigate the effects of these parameters on N_2O production pathways and emission rates during PN processes (Law et al., 2013, 2012, 2011; Pijuan et al., 2014; Wang

et al., 2014). Some studies have shown that N_2O emissions increased with decreasing DO concentration in a nitritation reactor receiving anaerobic sludge digestion liquor (Wang et al., 2014) and in a full-scale two-reactor PN–anammox process (Kampscheur et al., 2008). In contrast, other studies suggested that N_2O emissions increased with increasing DO concentrations in an AOB culture in a nitritation system fed with synthetic anaerobic digester liquor (Law et al., 2012) and pilot-scale anaerobic-anoxic-oxic (A2O) reactors (Furuya et al., 2013). Moreover, N_2O emissions were strongly dependent on pH in a highly enriched culture of AOB in a nitritation system fed with synthetic anaerobic digester liquor (Law et al., 2011).

In granular sludge, a steep concentration gradient is created towards the deeper part of the granule because the microbial density of granules is very high (Okabe et al., 2011b). As a result, the physicochemical parameters in the deeper parts of the granule are significantly different from those in the bulk liquid (Rathnayake et al., 2013; Song et al., 2013) and stratified distribution of microorganisms is created over a granule (Ishii et al., 2014). This can make the N_2O production and consumption processes in a granule more complicated and consequently might be responsible for various NERs among PN granular sludge processes. However, no studies have examined the effects of physicochemical parameters on N_2O production at the granular level. Accordingly, it is essential to investigate the N_2O production pathways and N_2O production rate *in situ* relative to local physicochemical conditions and microbial community structures in a granule to enhance understanding of N_2O emission mechanisms and then establish a strategy to mitigate N_2O

emissions in PN processes. Therefore, the present study was conducted to reveal (i) the effects of DO concentration and pH on N_2O production pathways and NERs of autotrophic PN granules taken from the autotrophic PN-sequencing batch reactor (SBR) (Rathnayake et al., 2013), (ii) the microbial community structure in PN granules, and (iii) the spatial distribution of the *in situ* N_2O production rate in PN granules. Based on these results, the effects of DO and pH on N_2O emission pathways and rates in the PN reactor were explained by the microbial community structure and the *in situ* N_2O production rate in the PN granules.

2. Materials and Methods

2.1 Batch experiments

Batch experiments were carried out using PN granules sampled from previously developed autotrophic PN-SBR (Rathnayake et al., 2013) to investigate the effects of DO concentration and pH on N_2O emissions from PN granules. All batch experiments were conducted in a laboratory bench-scale reactor with a working volume of 1.0 L and a headspace of 0.25 L. This batch reactor had the same configuration as the parent reactor except for the volume (see Figure S1 of the supplemental material). The synthetic medium for the batch experiments contained the same ingredients used in the autotrophic PN-SBR (Rathnayake et al., 2013), except for the concentrations of $(NH_4)_2SO_4$ (1050 mg L^{-1}, corresponding to 220 mg-N L^{-1}) and $NaNO_2$ (610 mg L^{-1}, corresponding to 124 mg-N L^{-1}). The NH_4^+ and NO_2^- concentrations corresponded to those

in the parent PN-SBR at 2 h after aeration started. A grab sample of the PN granules (3.0 g-volatile suspended solids (VSS)) was taken from the parent PN-SBR at 2 h after aeration started, washed three times with synthetic medium without NH_4^+ and NO_2^-, then re-suspended in 1.0 L of medium.

To investigate the effects of DO concentration on the NER of PN granules, batch tests were conducted at various DO concentrations (0.6, 1.1, 1.7 and 2.3 mg L^{-1}) and a fixed pH of 7.5 ± 0.05. DO was manually controlled by changing the ratio of N_2 gas and atmospheric air while the total gas flow rate was maintained at 150 ± 10 mL min^{-1}. To investigate the effects of pH on the NER of the PN granules, batch tests were conducted at different pH values (6.5, 7.0, 7.5, 8.0 and 8.5) while the DO concentration and the gas flow rate were fixed at 1.1 ± 0.1 and 2.0 ± 0.1 mg L^{-1} and 150 ± 10 mL min^{-1}, respectively. These DO concentrations and pH values for the batch tests were adopted based on the measured DO concentrations (0.8–2.5 mg/L) and pH values (6.3–8.5) in the parent PN-SBR. Each batch test was performed in triplicate. DO and N_2O concentrations and pH were continuously monitored until the N_2O emissions reached steady state (less than 40 min), which was defined as the point at which fluctuation in N_2O concentration for 5 min became less than 10% of the total change in N_2O concentration in a batch test. The bulk liquid samples in the batch reactor were collected at arbitrary time intervals and filtered using a 0.45-μm pore nitrocellulose membrane (Advantec, Tokyo, Japan). Concentrations of NH_4^+, NO_2^-, nitrate (NO_3^-) and DO and the pH of the liquid samples and N_2O concentration in the gaseous samples were

measured as described by Rathnayake et al. (2013). pH was controlled by adding HCl (0.5 M) or NaOH (0.5 M).

Allylthiourea (ATU) was used to distinguish the amount of N_2O produced by denitrification (nitrifier denitrification and heterotrophic denitrification) from that generated by nitrification (NH_2OH oxidation) in the batch experiments (Tallec et al., 2006). ATU inhibits aerobic oxidation of ammonia to NH_2OH by AOB. It was confirmed in advance that 10 mg-ATU L^{-1} completely inhibited the ammonia oxidation of the PN granules. N_2O produced in the batch test without ATU was defined as that produced via both nitrification and denitrification, whereas N_2O produced in the batch test with ATU was considered to be produced by denitrification alone. N_2O produced via nitrification was subsequently calculated by subtracting the amount produced by denitrification from that generated via both nitrification and denitrification. NER (mg-N g-VSS^{-1} h^{-1}) was calculated by multiplying the N_2O concentration in the off-gas by the gas flow rate and then dividing the product by the mass of the granules (g-VSS). The NH_4^+ oxidation rate (AOR) was calculated based on changes in NH_4^+ concentrations in a batch test and the mass of granules (g-VSS).

2.2 Microbial community structure in PN granules

Microbial community structure was analyzed by 16S rRNA gene amplicon deep sequencing conducted using the MiSeq technology (Illumina, Hayward, CA). Briefly, genomic DNA was

extracted from the PN granules (n=3) using a PowerSoil DNA Isolation kit (MoBio Technologies, Carlsbad, CA). The partial 16S rRNA gene sequences including the V3 and V4 regions were then amplified using primers Bakt_341F and Bakt_805R (Herlemann et al., 2011) with Illumina overhang adaptor sequences attached to their 5′ ends (Table S1). The reaction mixture (25 μL) contained 1× KAPA HiFi HotStart ReadyMix (Kapa Biosystems), 0.2 μM of each primer, and 2 μL of template cDNA. Polymerase chain reaction (PCR) was performed using a Veriti thermal cycler (Applied Biosystems, Foster City, CA) to subject the samples to the following conditions: initial annealing at 95°C for 3 min, followed by 25 cycles of 95°C for 30 s, 55°C for 30 s, and 72°C for 30 s. Twenty-five cycles of PCR were confirmed to be necessary and sufficient to reach the log-linear phase based on quantitative PCR analysis conducted using a KAPA SYBR Fast qPCR kit (Kapa Biosystems) and the Bakt_341F and Bakt_805R primers. The amplicons with Illumina overhang adaptor sequences were then purified using a LaboPass PCR Purification Kit (COSMO Genetech, Seoul, Korea), after which they were quantified with PicoGreen dsDNA quantification reagent (Molecular Probes, Eugene, OR, USA). The Illumina sequencing adaptor and index tag sequences were added to the amplicons using a Nextera XT Index kit (Illumina) according to the manufacturer's instructions, after which the resulting amplicons were purified using an AMPure XP kit (Beckman Coulter). Amplicons from triplicate samples were pooled in equal amounts and then purified again using a GeneRead Size Selection Kit (Qiagen). The resulting DNA was mixed with Phi X control DNA and employed as a template for paired-end sequencing using the MiSeq Reagent Kit v2 (500 cycles) and a MiSeq sequencer (Illumina).

Sequence reads from triplicate samples were analyzed using QIIME 1.8.0 (Caporaso et al., 2010) with the Silva 119 database. Representative sequences related to AOB were used to construct a phylogenetic tree based on the maximum-likelihood method using MEGA version 5 (Tamura et al., 2007).

2.3 Spatial distributions of AOB and N_2O producing activities in individual PN granules

The spatial distributions of betaproteobacterial AOB in single PN granules were determined by fluorescence in situ hybridization (FISH) (Rathnayake et al., 2013). Additionally, the steady-state concentration profiles of DO, N_2O and pH in the single PN granules were measured with microsensors at different DO concentrations or pH (Rathnayake et al., 2013). The granules were acclimated in the synthetic medium used for the batch experiment for at least 1 h before microsensor measurements to ensure that steady-state profiles were obtained. Physicochemical parameters of the medium were almost unchanged during the microsensor measurements. The net volumetric emission rates of N_2O ($R(N_2O)$) in the single granules were estimated from the concentration profile as previously described by Santegoeds et al. (1999).

3. Results and discussion

3.1 Effects of DO concentration on N_2O emissions from PN granules.

An increase in DO concentration from 1.1 mg L^{-1} to 2.3 mg L^{-1} at 20 min triggered an immediate

increase in N_2O concentration in the off-gas, and the N_2O concentration stabilized after 30 min (**Figure 1A**). The N_2O concentration decreased rapidly to the original concentration in response to decreasing DO concentration (2.3 mg L^{-1} to 1.1 mg L^{-1}). These results indicate that the impact of DO concentration on N_2O emissions from the PN granules was rapid and reversible. This DO-dependent N_2O emission phenomenon was highly reproducible (data not shown).

The effects of DO concentration on NER and AOR in the PN batch reactor were investigated at pH 7.5 based on the results of the batch tests described above. The AOR and NER increased linearly as DO concentration increased (**Figure 1B**). It should be noted that the relative fraction of N_2O emissions over the oxidized ammonia decreased from 2.9% (0.07 mg-N/2.4 mg-N) at 0.6 mg-DO L^{-1} to 1.4% (0.20 mg-N/14 mg-N) at 2.3 mg-DO L^{-1}.

The effects of DO concentration on N_2O production pathways (NH_2OH oxidation or denitrification (*i.e.*, nitrifier and heterotrophic denitrification)) in the PN granules were investigated using ATU as an inhibitor for aerobic ammonia oxidation. When the DO concentration was 0.6 mg L^{-1}, NER via nitrification was comparable to that via denitrification (**Figure 1C**). However, the NER via nitrification increased as the DO concentration increased. In contrast, the NER via denitrification was almost unchanged with increasing DO concentration. Plotting the NERs obtained from all batch tests against the corresponding AORs revealed a positive correlation ($r^2 = 0.71$) between these two parameters at AOR ranging from 0 to 20 mg-N

g-VSS^{-1} h^{-1}, suggesting that N_2O was produced via ammonium oxidation (**Figure 2**). These results agreed with those of a previous study of PN-SBR from which the PN granule samples were taken in this study that showed NH_2OH oxidation was responsible for up to 70% of the total N_2O emissions (Rathnayake et al., 2013).

3.2 Effects of pH on N_2O emissions from PN granules.

An increase in pH from 7.0 to 7.5 triggered an increase in the N_2O concentration of the off-gas with a 3 min time lag. The N_2O concentration reached a steady state N_2O concentration of 42 ppm at pH 7.5 within 30 min (**Figure 3A**). The N_2O concentration decreased in response to a decrease in pH from 7.5 to 7.0, reaching a steady state N_2O concentration of 20 ppm within 25 min. These findings indicate that the effects of changes in pH on N_2O emissions were reversible. More time was required to reach steady state in the experiments when pH was changed than when DO was changed.

The effects of pH on AOR and NER were investigated at DO 1.1 mg L^{-1} based on the results from the batch tests described above. The NER at pH 7.5 (0.15 ± 0.02 mg-N g-VSS^{-1} h^{-1}) was highest between pH 6.5 and 8.5 (**Figure 3B**). The relative fraction of N_2O emissions over the oxidized ammonia was also higher at pH 7.5 (2.5%) than at pH 6.5 (0.80%) and 8.5 (0.80%). In contrast, AOR were relatively constant between pH 6.5 and 8.5. Thus, there was no trend between AOR and NER (**Figure 2**).

The effects of pH on the N_2O production pathways in the PN granules were further investigated using 10 mg L^{-1} of ATU as an inhibitor for aerobic ammonia oxidation. The NERs via nitrification were higher than those via denitrification at all tested pH values (**Figure 3C**). Moreover, these values were highest at pH 7.5 (0.10 ± 0.02 mg-N^{-1} g-VSS^{-1} h^{-1}), which accounted for 80% of the total N_2O emissions (**Figure 3C**). The NER via denitrification decreased as pH increased. Specifically, the NER via denitrification at pH 8.5 (0.008 ± 0.001 mg-N g-VSS^{-1} h^{-1}) was four times lower than that at pH 6.5 (0.032 ± 0.01 mg-N^{-1} g-VSS^{-1} h^{-1}). Thus, the contribution of nitrification to the total N_2O emissions further increased to 85% at pH 8.5. The same trends were found at DO 2.0 mg L^{-1} in terms of AOR, NER and N_2O production pathways.

Similarly, previous studies demonstrated that N_2O emissions via heterotrophic denitrification increased as pH decreased (Okabe et al., 2011b). The higher N_2O emissions at lower pH ranges might be due to interference with N_2O reductase by free nitrous acid (FNA). Zhou et al. (2008) reported that 0.004 mg HNO_2-N L^{-1} of FNA completely inhibited N_2O reductase during denitrification. FNA concentration is a function of nitrite concentration, pH and temperature as described by the following equation (Qiao et al., 2010):

$$\mathrm{FNA(mg\,HNO_2 - N\,L^{-1})} = \frac{[\mathrm{NO_2^-} - \mathrm{N}]}{\mathrm{e}^{\left[\frac{-2300}{273+\mathrm{t}}\right]} \times 10^{\mathrm{pH}}}$$

FNA concentrations in the bulk liquid of the batch experiments were calculated to be 0.12 and 0.013 mg HNO_2-N L^{-1} at pH 6.5 and 7.5, respectively, using the above equation (see **Figure S2** in the supplemental material). These concentrations were high enough to completely inhibit N_2O reductase (Zhou et al., 2008). Increasing the pH led to decreased FNA concentrations (**Figure S2**), and consequently an increase in N_2O reducing activity, resulting in a decrease in NER via denitrification (**Figure 3C**).

3.3 Bacterial community structure in PN granules

The 16S rRNA gene deep sequencing analysis was conducted to examine the bacterial community structure in the PN granules, and a total of 290,157 sequences was obtained from triplicate samples (see Table S2 of the supplemental material). Microbial community structures were very similar among triplicate samples. AOB belonging to the bacterial order *Nitrosomonadales* were detected in high abundance (62.1 ± 5.6%) in autotrophic PN granules (**Figure 4A**), in which an operational taxonomic unit (OTU), PN1_7035 sequence (99.4% similar to *Nitrosomonas europaea* ATCC 19718 (GenBank accession NC_004757)), accounted for 60.5 ± 2.0% (**Figure 4B**). Another OTU, PN1_5365 (99.4% similar to the Bac02f3 clone retrieved from heterotrophic PN granules by Song et al., 2013), accounted for 20.5 ± 2.1%. These betaproteobacterial AOB were primarily detected in the oxic surface layer of the PN granules using a Nso1225 probe (**Figure S3**). Similar to the microbial community in the heterotrophic PN granules (Song et al., 2013), 16S rRNA gene sequences of potential denitrifiers such as *Burkholderiales* and

Rhodocyclales were also detected, but their abundances were low (11.5%).

3.4 Microsensor measurements

The *in situ* N_2O and DO concentrations and R(N_2O) in PN granules were measured at different DO concentrations and pH levels using microsensors (**Figure 5**). Regardless of the bulk DO concentrations (2 or 4 mg L^{-1}), oxic layers were limited to the upper 200 μm of the granules (**Figure 5A**), which agrees with the results of previous reports (Okabe et al., 1999, Song et al., 2013). The R(N_2O) calculated from the N_2O concentration profiles clearly indicated that N_2O production mainly occurs in the oxic layer (upper 200 μm) (**Figure 5B and D**). As the bulk DO concentrations increased, the N_2O production rates and the N_2O concentration inside the granules increased, mainly in the surface oxic layer.

These results indicated that increasing DO concentrations in the bulk liquid primarily stimulated N_2O production in the surface oxic layer. The FISH images and analysis of bacterial community structure showed that AOB, mainly *Nitrosomonas europaea*, were predominant in this layer. These findings indicated that N_2O might be produced by nitrification in the PN granules and that increases in DO in the bulk liquid predominantly stimulated N_2O production via nitrification in the surface oxic layer among the three N_2O production pathways. These *in situ* results clearly explained those of the batch tests (**Figures 1 and 2**), suggesting the importance of *in situ* analyses of PN granules to elucidate N_2O emission mechanisms in a PN process. In contrast to the

autotrophic PN granules, N_2O was produced by heterotrophic denitrifiers in the deeper anoxic parts (> 500 μm) of the heterotrophic PN granules, and the contribution of nitrification and nitrifier denitrification to N_2O emissions was relatively small (Ishii et al., 2014). Although nitrifier denitrification could not be distinguished from heterotrophic denitrification in the present study, N_2O production in the anoxic zones of the granules (**Figure 5B**) might be attributed to heterotrophic denitrification because N_2O is not produced via nitrifier denitrification under anoxic conditions (Kester et al., 1997; Yu et al. 2011). This may also have occurred because ammonium oxidation (*i.e.*, NH_2OH oxidation) by AOB does not occur under anoxic conditions and the density of AOB was very low in the anoxic zones (Rathnayake et al., 2013).

Higher *in situ* N_2O production was observed in the surface oxic layer of granules at pH 7.5 than at pH 6.5 and 8.5 (**Figure 5D**), which is consistent with the results of the batch experiments (**Figure 3**). The pH decreased slightly in the surface oxic layer owing to active ammonium oxidation (**Figure 5C**). Unlike the results of DO, the change in pH of the bulk liquid resulted in changes in pH throughout the granule. Therefore, changes in pH might affect N_2O production by both nitrification in the outer parts and denitrification in the inner parts of the granule (**Figure 3**).

N_2O production pathways and rates would be affected by other physicochemical parameters such as NO_2^- concentration (Kampschreur et al., 2008; Law et al., 2013), NH_4^+ loading rate (Ni and Yuan, 2013), and COD/N ratio (Kampschreur et al., 2009). Therefore, further studies are required

to determine the effects of NO_2^- and NH_4^+ concentrations and COD/N ratio on N_2O production mechanisms.

5. Conclusions

N_2O was mainly produced as a byproduct of nitrification by AOB belonging to the bacterial order *Nitrosomonadales* in the oxic surface layer of the autotrophic PN granules; therefore, increase in the bulk DO concentration stimulated ammonia oxidation and subsequently N_2O production. In PN granular sludge processes, N_2O is produced in microbial aggregates in which local physicochemical conditions differ greatly from those in bulk liquid. Therefore, it is essential to analyze *in situ* N_2O production and microbial community structures in relation to local physicochemical conditions to gain insight into N_2O emission mechanisms in PN processes.

Acknowledgments

This research was financially supported by grants from the Japan Science and Technology Agency (JST) CREST, Nagase Science and Technology Foundation, and Institute for Fermentation, Osaka (IFO) to S. Okabe. We thank Reiko Hirano and Ayumi Akiyoshi for their technical assistance.

References

1. Caporaso, J.G., Kuczynski, J., Stombaugh, J., Bittinger, K., Bushman, F.D., Costello, E.K., Fierer, N., Pentildea, A.G., Goodrich, J.K., Grordon, J.I., Huttley, G.A., Kelley, S.T., Knights, D., Koenig, J.E., Ley, R.E., Lozupone, C.A., McDonald, D., Muegge, B.D., Pirrung, M., Reeder. J., Sevinsky, J.R., Turnbaugh, P.J., Walters, W.A., Widmann, J., Yatsunenko, T., Zaneveld, J., Knight, R., 2010. QIIME allows analysis of high-throughput community sequencing data. Nat. Methods 7(5), 335–336.
2. Castro-Barros, C.M., Daelman, M.R.J., Mampaey, K.E., van Loosdrecht, M.C.M., Volck, E.I.P., 2015. Effect of aeration regime on N_2O emission from partial nitritation-anammox in a full-scale granular sludge reactor. Water Res. 68, 793–803.
3. Cho, S., Fujii, N., Lee, T., Okabe, S., 2011. Development of a simultaneous partial nitrification and anaerobic ammonia oxidation process in a single reactor. Bioresour. Technol. 102(2), 652-659.
4. Desloover, J., Vlaeminck, S.E., Clauwaert, P., Verstraete, W., Boon, N., 2012. Strategies to mitigate N_2O emissions from biological nitrogen removal systems. Curr. Opin. Biotech. 23(3), 474–482.
5. Furuya, Y., Saito, T., Konuma, S., Odake, Y., Suzuki, S., 2013. Effect of aeration intensity on nitrous oxide production. J. Water Environ. Technol. 11(6), 477–486.
6. Herlemann, D.P.R., Labrenz, M., Jurgens, K., Bertilsson, S., Waniek, J.J., Andersson, A.F., 2011. Transitions in bacterial communities along the 2000 km salinity gradient of the Baltic Sea. ISME J. 5, 1571–1579.

7. Igarashi, N., Moriyama, H., Fujiwara, T., Fukumori, Y., Tanaka, N., 1997. A structure of hydroxylamine oxidoreductase from a nitrifying chemoautotrophic bacterium, *Nitrosomonas europaea*. Nat. Struct. Mol. Biol. 4, 276–284.

8. Ishii, S., Song, Y., Rathnayake, L., Tumendelger, A., Satoh, H., Toyoda, S., Yoshida, N., Okabe, S., 2014. Identification of key N_2O production pathways in aerobic partial nitrifying granules. Environ. Microbiol. 16(10), 3168–3180.

9. Kampschreur, M.J., Temmink, H., Kleerebezem, R., Jetten, M.S.M., van Loosdrecht, M.C.M., 2009. Nitrous oxide emission during wastewater treatment. Water Res. 43(17), 4093–4103.

10. Kampschreur, M.J., van der Star, W.R.L., Wielders, H.A., Mulder, J.W., Jetten, M.S.M., van Loosdrecht, M.C.M., 2008. Dynamics of nitric oxide and nitrous oxide emission during full-scale reject water treatment. Water Res. 42(3), 812–826.

11. Kartal, B., Kuenen, J.G., van Loosdrecht, M.C.M., 2010. Sewage Treatment with Anammox. Science 328(5979), 702–703.

12. Kester, R. A.; de Boer, W.; Laanbroek, H. J., 1997. Production of NO and N_2O by pure cultures of nitrifying and denitrifying bacteria during changes in aeration. Appl. Environ. Microbiol. 63, 3872–3877.

13. Law, Y., Lant, P., Yuan, Z.G., 2011. The effect of pH on N_2O production under aerobic conditions in a partial nitritation system. Water Res. 45(18), 5934–5944.

14. Law, Y., Ni, B.-J., Lant, P., Yuan, Z., 2012. N_2O production rate of an enriched

ammonia-oxidising bacteria culture exponentially correlates to its ammonia oxidation rate. Water Res. 46(10), 3409–3419.

15. Law, Y., Lant, P., Yuan, Z., 2013. The confounding effect of nitrite on N_2O production by an enriched ammonia-oxidizing culture. Environ. Sci. Technol. 47, 7186–7194.
16. Lu, H.J., Chandran, K., 2010. Factors promoting emissions of nitrous oxide and nitric oxide from denitrifying sequencing batch reactors operated with methanol and ethanol as electron donors. Bioresour. Technol. 106(3), 390–398.
17. Ni, B., Yuan, Z., 2013. A model-based assessment of nitric oxide and nitrous oxide production in membrane-aerated autotrophic nitrogen removal biofilm systems. J. Membr. Sci. 428, 163–171.
18. Okabe, S., Oshiki, M., Takahashi, K., Satoh, H., 2011a. Development of long-term stable partial nitrification and subsequent anammox process. Bioresour. Technol. 102(13), 6801-6807.
19. Okabe, S., Oshiki, M., Takahashi, Y., Satoh, H., 2011b. N_2O emission from a partial nitrification-anammox process and identification of a key biological process of N_2O emission from anammox granules. Water Res. 45(19), 6461–6470.
20. Okabe, S., Satoh, H., Watanabe, Y., 1999. In situ analysis of nitrifying biofilms as determined by in situ hybridization and the use of microelectrodes. Appl. Environ. Microbiol. 65(7), 3182-3191.
21. Pijuan, M., Tora, J., Rodrıguez-Caballero, A., Cesar, E., Carrera, J., Perez, J., 2014. Effect

of process parameters and operational mode on nitrous oxide emissions from a nitritation reactor treating reject wastewater. Water Res. 49, 23–33.

22. Poughon, L., Dussap, C.G., Gros, J.B., 2001. Energy model and metabolic flux analysis for autotrophic nitrifiers. Biotechnol. Bioeng. 72(4), 416–433.

23. Qiao, S., Kawakubo, Y., Koyama, T., Furukawa, K., 2008. Partial nitritation of raw anaerobic sludge digester liquor by Swim-Bed and Swim-Bed activated sludge processes and comparison of their sludge characteristics. J. Biosci. Bioeng. 106(5), 433–441.

24. Rathnayake, R.M.L.D., Song, Y., Tumendelger, A., Oshiki, M., Ishii, S., Satoh, H., Toyoda, S., Yoshida, N., Okabe, S., 2013. Source identification of nitrous oxide on autotrophic partial nitrification in a granular sludge reactor. Water Res. 47, 7078–7086.

25. Santegoeds, C.M., Damgaard, L.R., Hesselink, C., Zopfi, J., Lens, P., Muyzer, G., De Beer, D., 1999. Distribution of sulfate-reducing and methanogenic bacteria in anaerobic aggregates determined by microsensor and molecular analyses. Appl. Environ. Microbiol. 65(10), 4618–4629.

26. Song, Y., Ishii, S., Rathnayake, L., Ito, T., Satoh, H., Okabe, S., 2013. Development and characterization of the partial nitrification aerobic granules in a sequencing batch airlift reactor. Bioresour. Technol. 139, 285–291.

27. Tallec, G., Garnier, J., Billen, G., Gousailles, M., 2006. Nitrous oxide emissions from secondary activated sludge in nitrifying conditions of urban wastewater treatment plants: Effect of oxygenation level. Water Res. 40(15), 2972–2980.

28. Tamura, K., Dudley, J., Nei, M., Kumar, S., 2007. MEGA4: molecular evolutionary genetics analysis (MEGA) software version 4.0. Mol. Biol. Evol. 24(8), 1596–1599.

29. Wang, Q., Jiang, G., Ye, L., Pijuan, M., Yuan, Z., 2014. Heterotrophic denitrification plays an important role in N_2O production from nitritation reactors treating anaerobic sludge digestion liquor. Water Res. 62, 202–210.

30. Wei, D., Shi, L., Zhang, G., Wang, Y., Shi, S., Wei, Q., Du, B., 2014. Comparison of nitrous oxide emissions in partial nitrifying and full nitrifying granular sludge reactors treating ammonium-rich wastewater. Bioresour. Technol. 171, 487–90.

31. Wrage, N., Velthof, G.L., van Beusichem, M.L., Oenema, O., 2001. Role of nitrifier denitrification in the production of nitrous oxide. Soil Biol. Biochem. 33(12-13), 1723–1732.

32. Yu, R., Kampschreur, M.J., van Loosdrecht, M.C.M., Chandran, K., 2010. Mechanisms and specific directionality of autotrophic nitrous oxide and nitric oxide generation during transient anoxia. Environ. Sci. Technol. 44(4), 1313–1319.

33. Zheng, Y.M, Yu, H.Q, Liu, S.H, Liu, X.Z., 2005. Formation and instability of aerobic granules under high organic loading conditions. Chemosphere 63(10), 1791–1800.

34. Zhou, Y., Pijuan, M., Zeng, R.J., Yuan, Z., 2008. Free nitrous acid inhibition on nitrous oxide reduction by a denitrifying-enhanced biological phosphorus removal sludge. Environ. Sci. Technol. 42(22), 8260–8265.

Figure legends

Figure 1. (**A**) Time-course profiles of DO concentration in the bulk liquid and N_2O concentration in the off-gas. (**B**) Effects of DO on N_2O production rate (NER) and ammonia oxidation rate (AOR). (**C**) The total NER and NERs via nitrification and denitrification at a variety of DO concentrations.

Figure 2. Correlation between ammonia oxidation rate (AOR) and N_2O production rate (NER) at a variety of DO concentrations and pH levels. The solid line indicates linear regression of the DO concentrations, which was given by the following equation: $y = 0.010x + 0.040$ ($r^2 = 0.71$).

Figure 3. (**A**) Time-course profiles of pH in the bulk liquid and N_2O concentration in the off-gas. (**B**) Effects of pH on the N_2O production rate (NER) and ammonia oxidation rate (AOR) at a variety of pH levels. (**C**) The total NER and NERs via nitrification and denitrification, and the contribution of nitrification and denitrification to N_2O production at a variety of pH levels.

Figure 4. (**A**) Microbial community composition of aerobic PN granules based on 16S rRNA gene sequences obtained by MiSeq sequencing. The inner, middle, and outer pie charts show the community composition at the phylum, order, and class levels, respectively. (**B**) Phylogenetic relationship between the representative AOB-related sequences obtained in this study (shown in

bold) and other AOB. The phylogenetic tree was constructed by the maximum-likelihood method using the 16S rRNA gene from *Nitrosococcus oceani* [NC_007484] as an outgroup for the tree. The accession numbers of the reference strains in the DDBJ/EMBL/GenBank databases are shown in brackets. The bootstrap values (>50%) derived from 1,000 replicates are indicated next to the branches.

Figure 5. (**A**) Steady-state concentration profiles of N_2O in PN granules at DO concentrations of 0 (●), 2 (▲), and 4 mg/L (■), and DO concentration profiles at DO concentrations of 2 (gray triangle) and 4 mg/L (gray square). (**B**) Net volumetric production rates of N_2O ($R(N_2O)$) in the single PN granules at DO concentrations of 0 (●), 2 (▲), and 4 mg/L (■). Positive and negative values indicate production and consumption rates, respectively. (**C**) Steady-state concentration profiles of N_2O (black points) and pH (gray points) profiles in the PN granules at pH 6.5 (●), 7.5 (▲) and 8.5 (■) in the bulk liquid. (**D**) $R(N_2O)$ in the single PN granules at pH 6.5 (●), 7.5 (▲), and 8.5 (■). Positive and negative values indicate production and consumption rates, respectively.

Figure S1. Schematic diagram of a bench-scale batch reactor. Liquid is circulated by air through an internal cylindrical plastic tube.

Figure S2. N_2O production rate (NER) and FNA concentration at various pH values. The dashed line indicates an FNA concentration of 0.004 mg-N L^{-1}.

Figure S3. Confocal laser-scanning microscope images of thin cross-section of a PN granule showing *in situ* spatial distribution of AOB (magenta) and other bacteria (blue) after fluorescence in situ hybridization using a Cy5-labeled EUB338 mix probe and TRITC-labeled Nso1225 probe. (For interpretation of the colors in this figure, see the web version of this article.)

Table S1. Primers used in this study.

Table S2. Similarity of microbial community compositions among triplicate samples, as determined by MiSeq 16S rRNA gene deep sequencing.

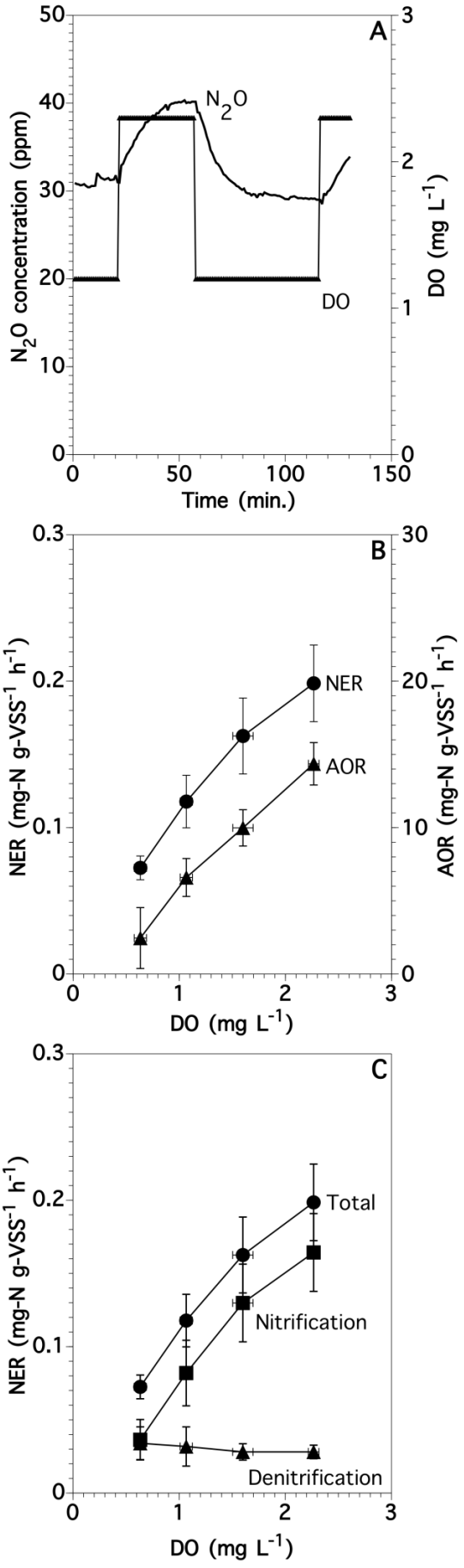


Figure 1. Rathnayake et al.

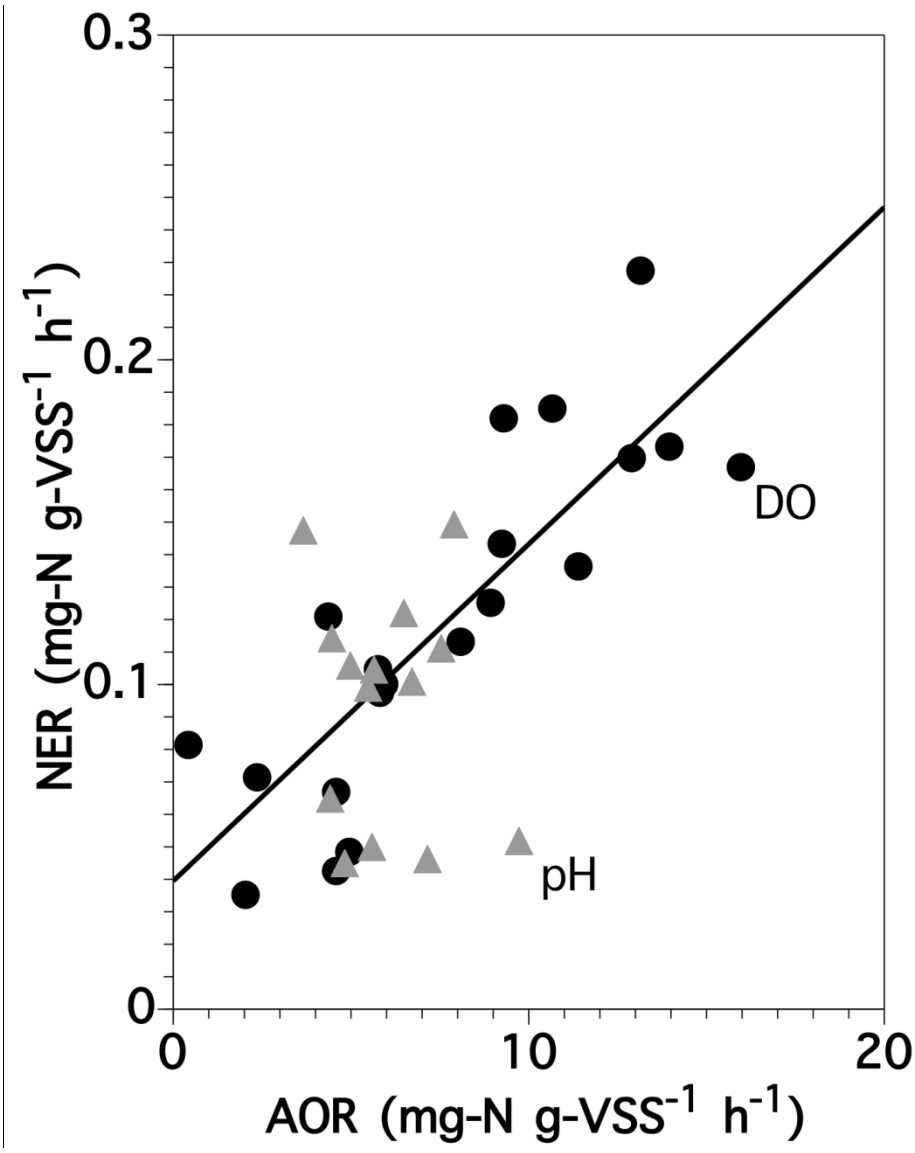


Figure 2. Rathnayake et al.

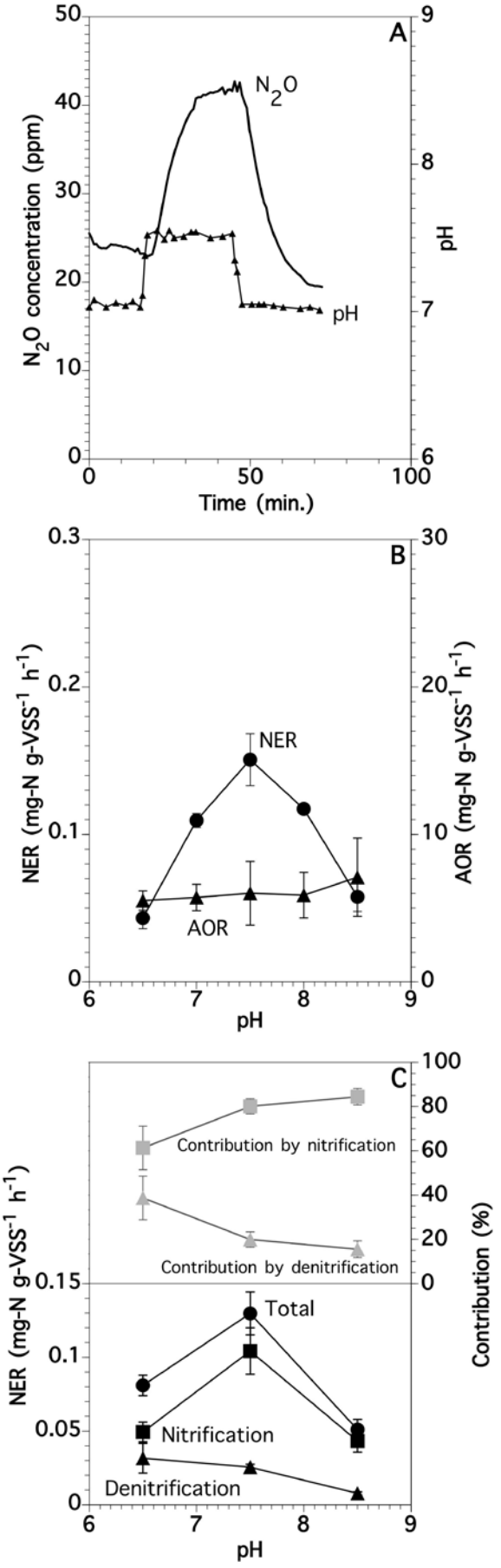


Figure 3. Rathnayake et al.

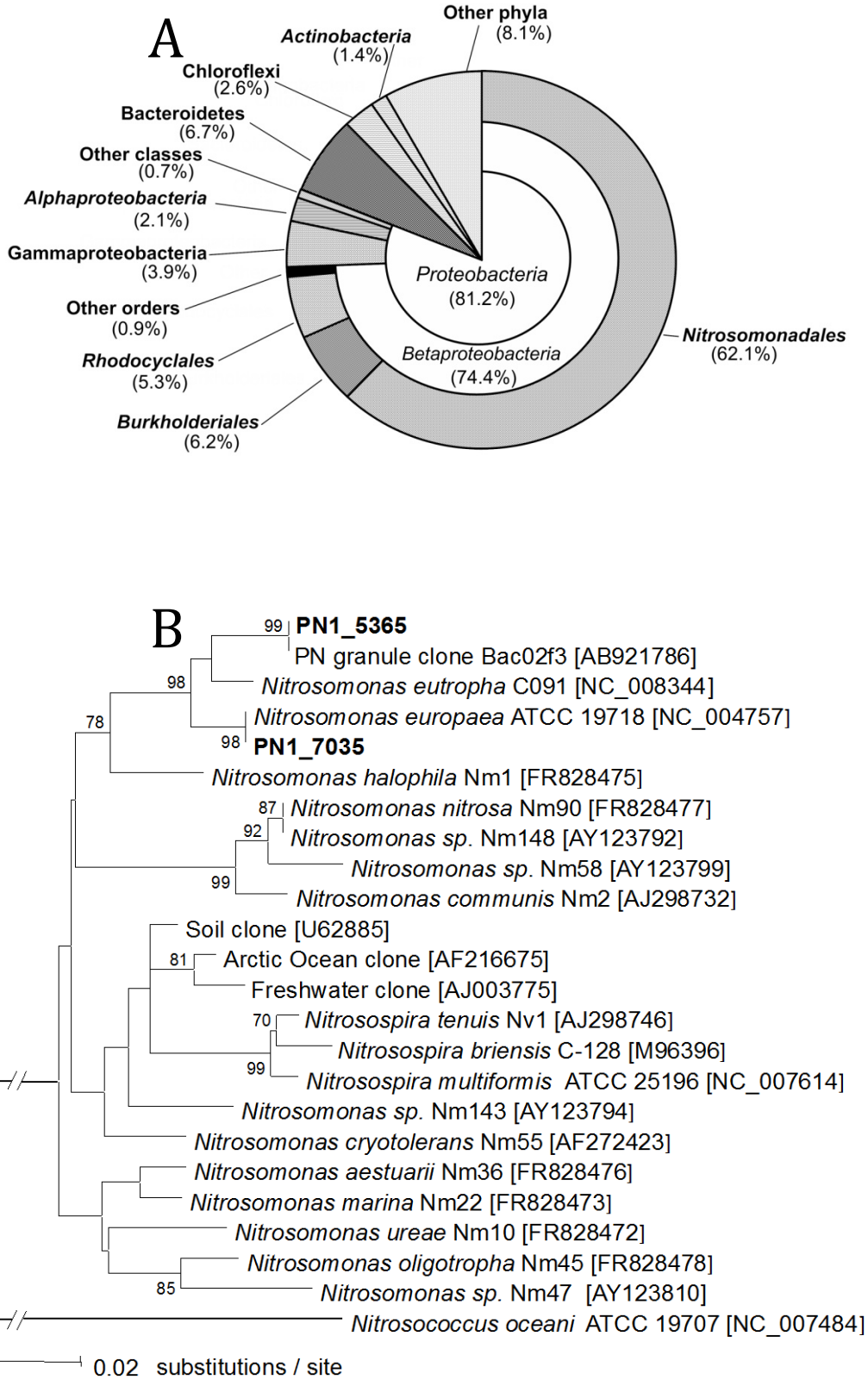


Figure 4. Rathnayake et al.

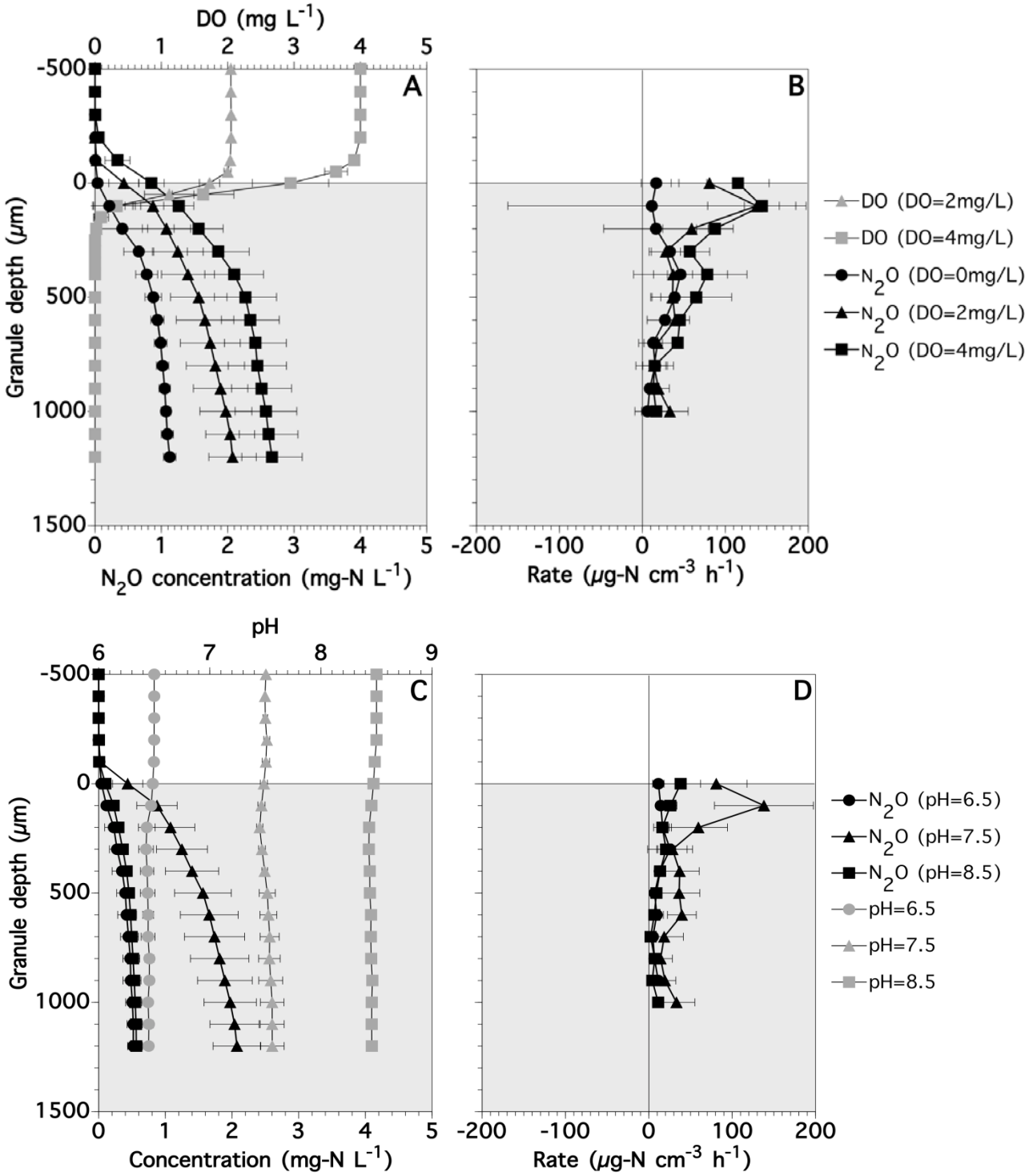


Figure 5. Rathnayake et al.